The Journal of Immunology

Epigenetic and Posttranscriptional Regulation of CD16 Expression during Human NK Cell Development

Aaron R. Victor, Christoph Weigel, Steven D. Scoville, Wing Keung Chan, Kelsey Chatman, Mary M. Nemer, Charlene Mao, Karen A. Young, Jianying Zhang, Jianhua Yu, Aharon G. Freud, Christopher C. Oakes and Michael A. Caligiuri

J Immunol 2018; 200:565-572; Prepublished online 11 December 2017;
doi: 10.4049/jimmunol.1701128
http://www.jimmunol.org/content/200/2/565

The Journal of Immunology is published twice each month by
The American Association of Immunologists, Inc.,
1451 Rockville Pike, Suite 650, Rockville, MD 20852

Print ISSN: 0022-1767 Online ISSN: 1550-6606.

Epigenetic and Posttranscriptional Regulation of CD16 Expression during Human NK Cell Development

Aaron R. Victor,[*,†,1] Christoph Weigel,[†,‡,1] Steven D. Scoville,[*,†] Wing Keung Chan,[†] Kelsey Chatman,[§] Mary M. Nemer,[§] Charlene Mao,[†] Karen A. Young,[†] Jianying Zhang,[¶] Jianhua Yu,[†,‡] Aharon G. Freud,[‖] Christopher C. Oakes,[†,‡,#,2] and Michael A. Caligiuri[†,‡,,2]**

The surface receptor FcγRIIIA (CD16a) is encoded by the *FCGR3A* gene and is acquired by human NK cells during maturation. NK cells bind the Fc portion of IgG via CD16a and execute Ab-dependent cell-mediated cytotoxicity, which is critical for the effectiveness of several antitumor mAb therapies. The role of epigenetic regulatory mechanisms controlling transcriptional and posttranscriptional CD16 expression in NK cells is unknown. In this study, we compared specific patterns of DNA methylation and expression of *FCGR3A* with *FCGR3B*, which differ in cell type–specific expression despite displaying nearly identical genomic sequences. We identified a sequence within the *FCGR3A* promoter that selectively exhibits reduced methylation in CD16a$^+$ NK cells versus CD16a$^-$ NK cells and neutrophils. This region contained the transcriptional start site of the most highly expressed CD16a isoform in NK cells. Luciferase assays revealed remarkable cell-type specificity and methylation-dependent activity of *FCGR3A*- versus *FCGR3B*-derived sequences. Genomic differences between *FCGR3A* and *FCGR3B* are enriched at CpG dinucleotides, and mutation of variant CpGs reversed cell-type specificity. We further identified miR-218 as a posttranscriptional negative regulator of CD16a in NK cells. Forced overexpression of miR-218 in NK cells knocked down CD16a mRNA and protein expression. Moreover, miR-218 was highly expressed in CD16a$^-$ NK cells compared with CD16a$^+$ NK cells. Taken together, we propose a system of *FCGR3A* regulation in human NK cells in which CpG dinucleotide sequences and concurrent DNA methylation confer developmental and cell type–specific transcriptional regulation, whereas miR-218 provides an additional layer of posttranscriptional regulation during the maturation process. ***The Journal of Immunology*****, 2018, 200: 565–572.**

The low-affinity FcγRIIIA (or CD16a) is an activating Fc receptor expressed by NK cells, macrophages, and monocytes. It is coded by the gene *FCGR3A*. Surface expression of CD16a is required for Ab-dependent cell-mediated cytotoxicity (ADCC). The efficacy of several clinically effective antitumor Abs involves the engagement of CD16a, which is required for ADCC (1–5). CD16a expression is acquired during NK cell maturation, which can be described in five sequential stages involving NK cell developmental intermediates (NKDIs) (6). Stages 1–3 are considered progenitor or immature stages and do not express CD16a. Stages 4 and 5 NK cells are considered mature. Expression of CD16a divides stage 4 (early mature) and stage 5 (late mature) NK cells (7–9). The NK cell population in secondary lymphoid tissues (SLTs) is primarily composed of CD16a$^-$ NKDIs, including stage 4 NK cells, which are characterized by the CD56^{bright}/CD16a$^-$ surface phenotype. SLTs also contain a minor population that is CD56$^+$/CD16a$^+$ and corresponds to a stage 5 NK cell phenotype. In the peripheral blood, this pattern is reversed: CD56^{bright}/CD16a$^-$ stage 4 NK cells are the minor population, whereas CD56^{dim}/CD16a$^+$ stage 5 NK cells are the predominant population. This suggests that CD56^{bright}/CD16a$^-$ NKDIs develop in SLTs before full maturation and traffic into the periphery as stage 5 NK cells (7). Although the function of this receptor has been well characterized (3, 10–18), and its post-translational regulation has been described (19), the mechanism(s) of *FCGR3A* regulation permitting the developmental acquisition of CD16a is not understood.

The lack of knowledge regarding *FCGR3A* regulation during human NK cell development is due, in part, to inherent difficulties in studying this gene. Cell lines expressing CD16a are notably

*Medical Scientist Training Program, The Ohio State University, Columbus, OH 43210; †The Ohio State University Comprehensive Cancer Center, Arthur G. James Cancer Hospital and Richard J. Solove Research Institute, Columbus, OH 43210; ‡Division of Hematology, Department of Internal Medicine, The Ohio State University, Columbus, OH 43210; §College of Medicine, The Ohio State University, Columbus, OH 43210; ¶Center for Biostatistics, Department of Bioinformatics, The Ohio State University, Columbus, OH 43210; ‖Department of Pathology, The Ohio State University, Columbus, OH 43210; #Department of Biomedical Informatics, The Ohio State University, Columbus, OH 43210; and **Department of Cancer Biology and Genetics, The Ohio State University, Columbus, OH 43210

[1]A.R.V. and C.W. contributed equally to this work.

[2]C.C.O. and M.A.C. are cosenior authors.

ORCIDs: 0000-0003-4118-3088 (A.R.V.); 0000-0002-5257-1521 (W.K.C.); 0000-0001-9490-0058 (K.C.); 0000-0002-5517-7183 (C.M.).

Received for publication August 7, 2017. Accepted for publication November 6, 2017.

This work was supported by the National Institutes of Health (Grants CA095426, CA210087, CA163205, CA199447, CA068458, and CA09338) and by the Ohio State University Comprehensive Cancer Center.

The microarray data presented in this article have been submitted to the Gene Expression Omnibus (https://www.ncbi.nlm.nih.gov/geo) under accession number GSE106469.

Address correspondence and reprint requests to Dr. Michael A. Caligiuri and Dr. Christopher C. Oakes, Division of Hematology, Department of Internal Medicine, The Comprehensive Cancer Center, The Ohio State University, 320 West 10th Avenue, Columbus, OH 43210. E-mail addresses: Michael.Caligiuri@osumc.edu (M.A.C.) and Christopher.Oakes@osumc.edu (C.C.O.)

The online version of this article contains supplemental material.

Abbreviations used in this article: ADCC, Ab-dependent cell-mediated cytotoxicity; ATCC, American Type Culture Collection; miRNA, microRNA; NKDI, NK cell developmental intermediate; Pmed1, medial promoter-1; Pprox, proximal promoter; rhIL-2, recombinant human IL-2; SLT, secondary lymphoid tissue; UTR, untranslated region.

lacking (20). The closest murine genes, *Fcgr3* and *Fcgr4*, have limited homology (<50%) to human *FCGR3A*. Furthermore, in humans, a recent genomic segmental duplication event generated two genes, *FCGR3A* and *FCGR3B*, that retain a very high degree of sequence homology (>95%) across the gene locus (21). Abs that recognize CD16 generally recognize both gene products. Discrimination of these two homologs is highly relevant to immunological studies, because *FCGR3B* cannot mediate ADCC and instead functions as a sink for immune complexes (21, 22).

Despite their nearly identical genomic sequences, FCGR3 homologs are selectively expressed by specific cell types; *FCGR3A* is expressed by NK cells, monocytes, and macrophages, whereas *FCGR3B* is expressed by neutrophils (21). Previous work has shown that each FCGR3 homolog uses two distinct alternative promoters within its respective 5′-region to transcribe at least two unique transcripts (23, 24). In *FCGR3A*, both promoters confer selective activity in the NK cell line YT, whereas the *FCGR3B* promoter alternatively operates myeloid cells, indicating that lineage-specific factors are capable of selectively recognizing sequence differences between FCGR3 homologs (23, 24). However, the mechanism that endows this exquisite specificity and how it selectively develops in separate primary cell lineages are not understood.

To gain insight into mechanisms that might regulate *FCGR3A*, we focused our studies on NK cells. Epigenetic gene regulation is capable of tightly controlling gene expression in a developmental- and tissue-specific manner (25, 26) and may help to explain the tissue specificity, despite the very high degree of homology between *FCGR3A/B*. NKDIs do not quickly acquire CD16a surface expression, often requiring a week or more of expansion in vitro before significant CD16a expression is detectable by flow cytometry (27, 28). As the cells acquire CD16a expression, some level of posttranscriptional fine-tuning may also be required. To address this possibility, we further sought to identify microRNA (miRNA) regulators of *FCGR3A*.

In this article, we identify two types of regulation of CD16a in human NK cells: DNA methylation of the *FCGR3A* promoter and miR-218 targeting of *FCGR3A* mRNA. These mechanisms suggest that CD16a expression in repressed in stage 4 NK cells, primarily by DNA methylation silencing with concurrent high miR-218 expression. The time required to transition from stage 4 to stage 5 may be necessary to sufficiently modify the *FCGR3A* promoter methylation patterns and downregulate miR-218, culminating in robust CD16a expression in stage 5 NK cells.

Materials and Methods

Isolation of primary human cells from peripheral blood

All human cell work was performed with approval of The Ohio State University Institutional Review Board. Human NK cells were isolated from peripheral blood leukopaks of healthy individuals (American Red Cross) by negative selection with a MACSxpress NK Cell Isolation Kit, human (Miltenyi Biotec). Enriched cells were collected and labeled for FACS sorting. For DNA isolation of $CD16^-$ and $CD16^+$ NK cells, we gated on lymphocyte, followed by $CD3^-CD56^+$ gating, and then sorted for $CD56^{bright}CD16^-$ or $CD56^{dim}CD16^+$ populations, respectively. NK cells were sorted to >95% purity. Human neutrophils were enriched with CD66abce magnetic beads by positive selection (Miltenyi Biotec). Enriched cells were labeled for FACS with CD15 and CD16 Abs. For DNA isolation, we gated on the $CD15^+CD16^+$ population. Cells were sorted to >97% purity.

Abs and flow cytometric analysis

The following Abs were used to stain human peripheral blood cells: CD3 (SK7; BD Biosciences), CD14 (TÜK4; Miltenyi Biotec), CD15 (VIMC6; Miltenyi Biotec), CD16 (VEP13; Miltenyi Biotec), CD16 (3G8; BD Biosciences), and CD56 (N901; Beckman Coulter). Flow cytometry data were analyzed with FlowJo v7.6.1 (TreeStar).

Cell culture

YT (American Type Culture Collection [ATCC]), K562 (ATCC), and Jurkat (German Collection of Microorganisms and Cell Cultures) cells were cultivated in RPMI 1640/10% FBS (Life Technologies) and supplemented with Antibiotic-Antimycotic (Thermo Fisher Scientific). NKL cells were cultivated in RPMI 1640/10% FBS (Life Technologies) and supplemented with Antibiotic-Antimycotic (Thermo Fisher Scientific) and 150 IU/ml recombinant human IL-2 (rhIL-2) (Roche). HEK293T cells were obtained from the ATCC. HEK293T cells were cultured in DMEM/10% FBS (Life Technologies) and supplemented with antibiotics.

Quantitative DNA methylation analysis using MassARRAY

DNA was isolated using a Puregene Core Kit B (QIAGEN). One microliter of molecular-grade glycogen (Thermo Fisher Scientific) was added to each sample, and DNA was allowed to precipitate overnight at −20°C, followed by resuspension in water. DNA methylation analysis of the CD16 loci was carried out using the MassARRAY EpiTYPER assay (Agena Biosciences) (29). In short, genomic DNA was subjected to bisulfite treatment using an EZ DNA methylation kit (Zymo Research). Regions of interest were amplified with PCR primers specific for the *FCGR3A* or *FCGR3B* gene loci (primers are listed in Supplemental Table I) using the hg19 genome assembly from the UCSC Genome Browser (https://genome.ucsc.edu) (30). PCR products were transcribed in vitro and fragmented with RNase A (Agena Biosciences) to generate oligonucleotides that were subsequently analyzed via MALDI-TOF mass spectrometry. Ratios of unmethylated versus methylated oligonucleotide signals were used to calculate the percentage of DNA methylation for individual CpG dinucleotides. To examine the specificity of *FCGR3A* and *FCGR3B* assays, amplified sequences included non-CpG sequence variants that produced quantifiable differences in the mass spectra. Primers used for the final analysis were determined to be highly specific.

Luciferase reporter assay

Luciferase reporter assays were carried out as described previously (31). Sequences of the *FCGR3A* and *FCGR3B* 5′ untranslated regions (UTRs) were amplified using PCR and primers specific for each gene (listed in Supplemental Table I) and inserted into the CpG-free reporter vector pCpGfree-promoter-Lucia (InvivoGen). Sequences were verified with Sanger Sequencing at the Plant-Microbe Genomics Facility (The Ohio State University). For methylation-specific assays, plasmids were methylated in vitro using CpG Methyltransferase (M.SssI) (Thermo Fisher Scientific). Luciferase assays were carried out in HEK293T cells using TransIT-LT1 Transfection Reagent (Mirus Bio), according to the manufacturer's instructions. Jurkat, YT, and K562 cells were transfected with a Nucleofector device (Lonza) using an Amaxa Cell Line Nucleofector Kit V with programs X-001, O-017, and T-016, respectively. Luciferase activity was assessed 48 h after transfection on a DTX880 Multimode Detector (Beckman Coulter). Luciferase signals were normalized to cotransfected pGl4–CMV–firefly luciferase vector (Promega). Luciferase activity values were displayed relative to an unmodified pCpGfree-promoter-Lucia plasmid.

RNA isolation, miRNA-expression assays, and real-time PCR

Total RNA from the indicated cell types was extracted using the Total RNA Purification Plus Kit (Norgen Biotek). For miRNA analysis, we used an nCounter miRNA Expression Assay (NanoString Technologies) interrogating a panel of 800 miRNAs. The microarray data presented in this article have been submitted to the Gene Expression Omnibus (https://www.ncbi.nlm.nih.gov/geo) under accession number GSE106469. miRNA expression was also determined using TaqMan MicroRNA Assays (Thermo Fisher Scientific). cDNA from mRNA was generated using a SuperScript VILO cDNA Synthesis Kit (Thermo Fisher Scientific) or SuperScript III reverse transcriptase (cell lines). Real-time PCR was done using Power SYBR Green Master Mix reagent (Thermo Fisher Scientific) and a ViiA 7 Real-Time PCR System (Applied Biosystems). Relative gene expression was calculated as $2^{-\Delta ct}$, with Δct = (ct target − ct housekeeping gene), where ct stands for threshold cycle. Data were individually normalized to housekeeping gene expression values of β-actin, GAPDH, TATA box binding protein, and hypoxanthine phosphoribosyltransferase 1; the average of the four normalized expression values was used per sample. Quantitative assessment of the ratio of *FCGR3A*/*FCGR3B* expression was performed using the MassARRAY iPLEX application (Agena Biosciences) designed for the accurate measurement of allele-specific expression (32). Briefly, five primer sets were used to amplify cDNA from purified $CD16^+$ NK cells and neutrophils that targeted *FCGR3A* and *FCGR3B* equally, but flanked at least one discriminatory nucleotide (primers are listed in

Supplemental Table I). Oligonucleotides were annealed to the PCR products immediately 5′ to the discriminatory nucleotide, followed by single-base extension. Mass spectrometry was used to determine the ratio of *FCGR3A*/*FCGR3B* sequences; the reported values represent the average of the five assays.

Lentiviral infection of primary human NK cells

Infections were modified from a previously published protocol (33). Briefly, low-passage (5–20) HEK293T cells were transfected with pCDH CD511B-1 (System Biosciences) and two packaging plasmids containing VSV-G and *gag/pol/tat/rev*. pCDH expression vectors contained no insert or *mir-218-2* plus 200 bp upstream and downstream. Virus media were concentrated by centrifugation (20,000 × *g*). Human NK cells isolated by FACS sorting were cultured overnight in RPMI 1640/5% human AB serum/Antibiotic-Antimycotic supplemented with 450 IU/ml rhIL-2. NK cells were infected with virus in 96-well round-bottom plates at a multiplicity of infection of 2–10. Plates were centrifuged for 2 h at 1800 rpm at 32°C and placed in a 37–C incubator overnight. After resting the cells in virus-free media, NK cells were subjected to a second round of infection with virus overnight. The next day, virus media were removed again and replaced with RPMI 1640/5% human AB serum/Antibiotic-Antimycotic supplemented with 450 IU/ml rhIL-2, and cells were cultured for 48 h. NK cells were stained, sorted for live GFP$^+$ cells, and used for RNA expression assays.

Results

DNA methylation analysis of FCGR3A

NK cells acquire CD16a as part of their maturation process; less mature NK cells tend to be found in SLTs such as the lymph nodes and more mature NK cells tend to be found in the peripheral blood. To study the acquisition of CD16a by NK cells, we sorted NK subpopulations that precede and succeed this process and obtained CD16a$^-$ and CD16a$^+$ subpopulations at >95% purity (Fig. 1). We next assessed DNA methylation of the proximal promoter region of *FCGR3A* in these NK cell subsets. Because *FCGR3B* displays a different tissue-specific expression pattern, yet a high degree of promoter sequence homology compared with *FCGR3A*, we included both genes in our analysis to identify important regulatory features. *FCGR3A* and *FCGR3B* genes are separated by ~81 kb on chromosome 1q23.3 and show nearly identical exon/intron architectures and promoter sequences (Fig. 2A). Both genes are annotated in the RefSeq database as being potentially expressed from at least two alternative transcriptional start sites: transcript variants 1 and 3 for *FCGR3A* and variants 1 and 2 for *FCGR3B* (with variants 3 and 2 being homologous between *FCGR3A* and *FCGR3B*, respectively). There are two promoters annotated for *FCGR3A*: proximal promoter (Pprox)-A (−198 to −10 bp) and medial promoter-1 (Pmed1)-A (−942 to −850 bp) (23, 24). Corresponding regions in *FCGR3B* were termed Pprox-B and Pmed1-B. To separately interrogate the profile of DNA methylation across both genes, we used the quantitative MassARRAY system and PCR primers that exploit sequence variations between *FCGR3A* and *FCGR3B* genes. Analysis of primary sorted CD16a$^+$ and CD16a$^-$ NK cell subsets revealed that CD16a$^+$ NK cells show lower methylation levels within the *FCGR3A* 5′-region compared with CD16a$^-$ NK cells (Fig. 2B). CpGs exhibiting the greatest difference between subsets were focused in Pmed1-A and immediate downstream sequences. The Pprox-A region was partially unmethylated in CD16a$^-$ NK cells, whereas the region in the vicinity of Pmed1-A only showed low methylation in CD16a$^+$ NK cells. *FCGR3B* was highly methylated throughout the entire 5′ region in CD16a$^-$ and CD16a$^+$ NK cells, consistent with selective expression of *FCGR3A* in the NK lineage (21). We next investigated the NK cell lines YT and NKL, which are negative and positive for FCGR3A mRNA, respectively. YT cells generally showed high methylation of *FCGR3A* (and *FCGR3B*), whereas NKL cells showed lower levels of methylation in *FCGR3A*, including CpGs immediately proximal and within Pmed1-A (Fig. 2C). These data show that pronounced lower

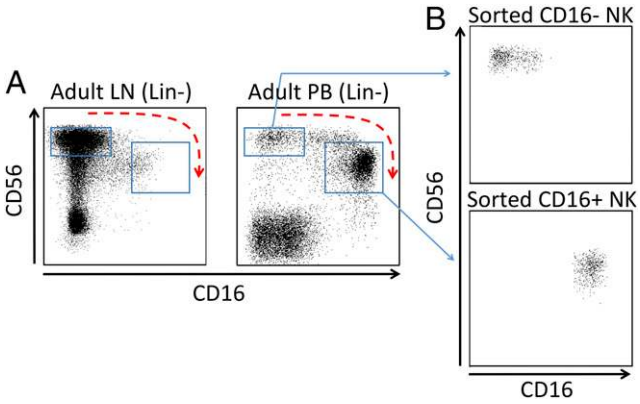

FIGURE 1. NK cells acquire CD16a during normal maturation. (**A**) Mononuclear cells from adult axillary lymph node (LN) and adult peripheral blood (PB) were analyzed by flow cytometry by gating on Lin$^-$ cells and then NK cell markers CD56 and CD16a. Blue boxes indicate CD56^{bright}/CD16a$^-$ NK cells and CD56^{dim}/CD16a$^+$ NK cells. Curved red dashed arrows indicate the presumed pathway of normal CD16a acquisition by NK cells. (**B**) Straight blue arrows designate the sorted NK cell populations used in DNA methylation analyses.

levels of DNA methylation are found at the *FCGR3A* promoter versus the *FCGR3B* promoter in CD16a$^+$ NK cells, and differential surface expression of CD16a is associated with reduced methylation of CpGs surrounding the Pmed1-A promoter.

To further investigate the role of DNA methylation in the selective expression of *FCGR3A*, we sorted primary neutrophil samples, which selectively express *FCGR3B* (21). We found that CpGs in the *FCGR3A* promoter that selectively demonstrated low methylation in CD16a$^+$ NK cells were highly methylated in neutrophils, whereas two regions of low methylation in *FCGR3B* were observed (Fig. 2D). These regions corresponded to Pprox-B and CpGs adjacent to, but not within, Pmed1-B. Similar to CD16a$^-$ NK cells, neutrophils also displayed low methylation of Pprox-A within *FCGR3A*, despite both cell types lacking expression of *FCGR3A*. These data show that, in neutrophils, the selective expression of *FCGR3B* is associated with a decrease in *FCGR3B* methylation, primarily at Pprox-B, corresponding to the known promoter usage (34), and, like CD16a$^-$ NK cells, low methylation of Pprox-A is not associated with expression.

Promoter-specific DNA methylation is associated with FCGR3A/B variant expression

To demonstrate the importance of methylation differences between transcriptional start sites, we next evaluated the expression of the transcript variants within *FCGR3A* and *FCGR3B* genes in primary cells. Because the 5′ exon sequences of *FCGR3A* and *FCGR3B* are virtually identical, the sequence identity between genes does not allow the discrimination of variant expression from each gene promoter individually. Thus, we first ensured that the relative expression of *FCGR3A* versus *FCGR3B* in our samples matched reported cell type–specific expression patterns. For this, we measured the expression of *FCGR3A* relative to *FCGR3B* using a highly quantitative and accurate MassARRAY method for determining transcript expression ratios (32). We confirmed that CD16a$^+$ NK cells are virtually only expressing *FCGR3A*, and neutrophils are expressing only *FCGR3B* (Fig. 2E). Next, using quantitative RT-PCR primers that are specific for variant 1 (*FCGR3A* and *FCGR3B*) or variants 3 (*FCGR3A*) and 2 (*FCGR3B*), we found that CD16a$^+$ NK cells are strongly expressing variant 3 (and variant 1, to some extent); inversely, neutrophils are strongly expressing variant 1 and a small amount of variant 2 (Fig. 2F). Taken together, these data show that primary CD16a$^+$ NK cells primarily use the Pmed1-A

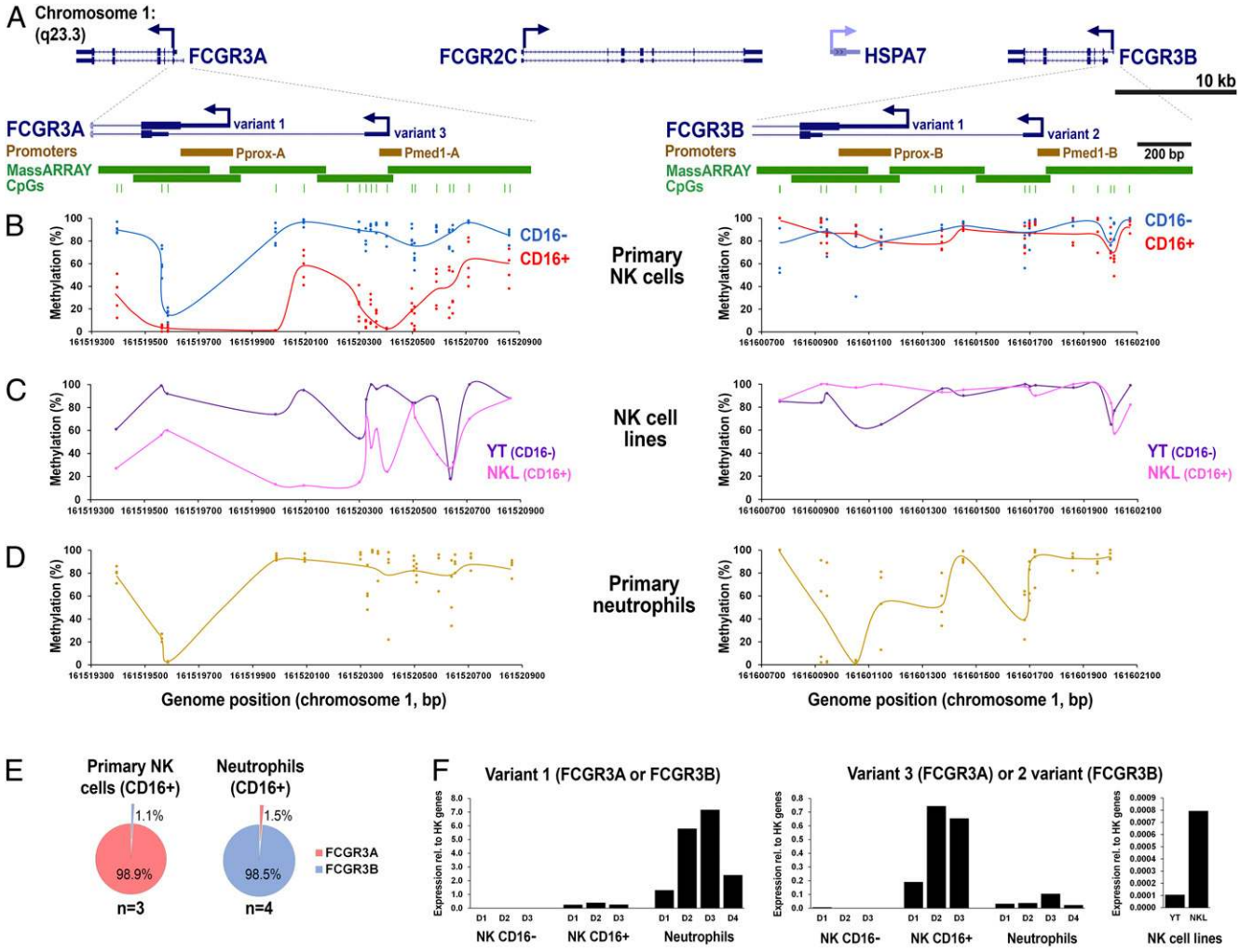

FIGURE 2. DNA methylation and isoform-specific expression within the promoter regions of *FCGR3A* and *FCGR3B*. (**A**) Representation of the FCGR3 locus spanning ~100 kb of chromosome 1q23.3 displaying transcripts annotated in the RefSeq database (adapted from the UCSC Genome Browser) (upper panels). Promoter regions of *FCGR3A* and *FCGR3B* are enlarged, displaying the various transcript variants annotated in the RefSeq database that differ in the 5′ region (lower panels). MassARRAY amplicons (green bars) used are shown along with the positions of CpG dinucleotides (green markers). (**B**) The MassARRAY EpiTYPER assay was used to interrogate the DNA methylation levels of CpGs across the promoter region of *FCGR3A* and *FCGR3B* in a gene-specific manner in sorted NK CD16a$^+$ and CD16a$^-$ fractions. Methylation plots are aligned to enlargements of gene promoters according to the hg19 genome assembly. DNA methylation levels in NK cell lines (**C**) and neutrophils (**D**). (**E**) Expression ratio of *FCGR3A*/*FCGR3B* in CD16a$^+$ NK cells and neutrophils, as determined by the MassARRAY iPLEX assay. (**F**) Quantitative RT-PCR analysis of 5′ transcript variants using primers specific for variant 1 or variants 3 and 2, indicating promoter usage in NK cells, neutrophils, and NK cell lines YT and NKL (both primer pairs do not distinguish *FCGR3A* from *FCGR3B*). D1–4 represents donors 1–4. Expression values are relative to the average of four housekeeping (HK) genes. TSS, transcriptional start site.

promoter, whereas neutrophils mainly use Pprox-B, similar to previous observations in cell lines (23).

Specific activity of Pmed1-A/B is silenced by DNA methylation

To functionally evaluate the role of DNA methylation in the control of the selective activity of *FCGR3A* and *FCGR3B* variant promoters, the proximal 5′ region from each gene was split into four sections and cloned individually into a promoter-less luciferase-expressing plasmid devoid of CpG dinucleotides (Fig. 3A). Luciferase plasmids were transfected into YT cells (NK lineage), K562 cells (myeloid lineage), and into Jurkat and HEK293T cells as negative controls for non–CD16a-expressing lineages. As found previously (23, 24, 35), the Pmed1-A region, but not Pmed1-B, was selectively activated in YT cells (Fig. 3B). K562 cells selectively activated Pmed1-B, but not Pmed1-A. Other cloned regions did not possess inherent promoter activity in either lineage, including Pprox promoters that are known to require additional flanking enhancer sequences (23, 24). Importantly, in vitro methylation of Pmed1 sequences abolished their activity in both lineages (Fig. 3B), corroborating the findings in primary cells that DNA methylation of Pmed1-A is likely involved in the regulation of CD16a expression in the NK lineage.

Selective activity of Pmed1-A/B requires specific CpG dinucleotides

To identify the basis for lineage-specific expression of Pmed1, we aligned Pmed1-A and Pmed1-B sequences and found that variants are strongly enriched at CpG dinucleotides. Differences generally disrupt CpGs in *FCGR3B* versus *FCGR3A*, including CG > TG transitions at CpG1 and CpG2 and an 8-bp indel that disrupts CpG6 (Fig. 3C). To test whether these CpGs are involved in selective regulation, we introduced C > T mutations for CpG1 and CpG2 in Pmed1-A *FCGR3A*, which enhances the likeness toward *FCGR3B*, and then retested these regions in our luciferase-based expression assay (Fig. 3D). Mutation of these CpGs abolished selective activity in YT cells. Remarkably, these mutations permitted Pmed1-A to be

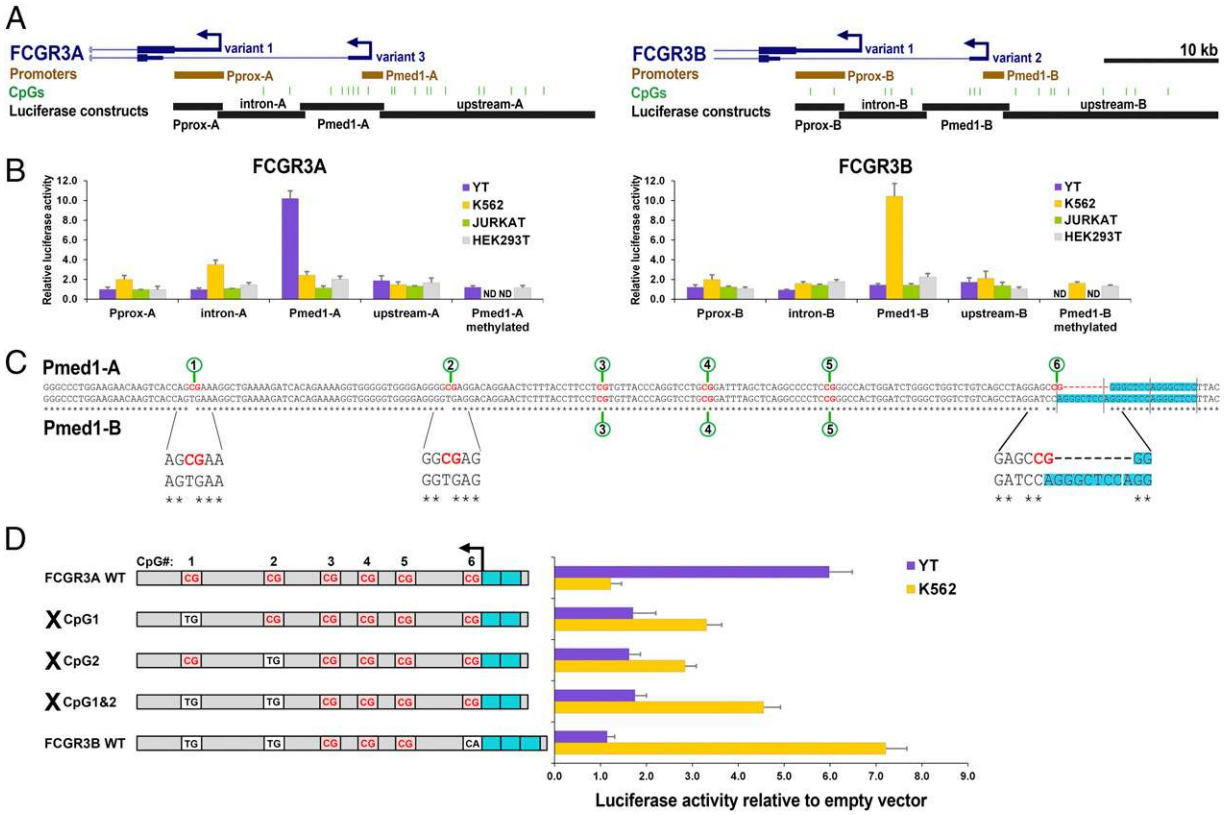

FIGURE 3. Analysis of DNA methylation- and lineage-specific activity of FCGR3 promoter sequences. (**A**) Illustration of *FCGR3A* and *FCGR3B* sequences cloned into luciferase constructs (black bars). (**B**) Four promoter sequence fragments were cloned from *FCGR3A* (left panel) or *FCGR3B* (right panel) and transfected into various cell lines. Luciferase assays showing sequence- and gene-specific activity (relative to empty vector control). Pmed1-A and Pmed1-B were also methylated in vitro prior to transfection. Error bars represent SEM of $n = 3$ individual experiments. (**C**) Sequence alignment of Pmed1-A and Pmed1-B with numbered CpGs. All sequence variants are enlarged below; an 8-bp repeat occurring in the vicinity of CpG6 is highlighted in blue, and asterisks below the sequence indicate homology. (**D**) Luciferase activity following site-directed mutagenesis of CpG1 and CpG2 of Pmed1-A compared with unaltered *FCGR3A* and *FCGR3B* sequences in YT and K562 cells. ND, not done.

expressed in K562 cells, because increased likeness toward *FCGR3B* in the pattern of CpG sequences was associated with increased activity in K562 cells. This suggests that, in addition to the regulatory function provided by CpG methylation, the CpGs themselves are required to direct selective expression of *FCGR3A* versus *FCGR3B*.

Prediction of miRNAs that target FCGR3A

To identify miRNA regulators of *FCGR3A*, we followed the strategy described by Witkos et al. (36). We compiled a list of 53 potential miRNA regulators by using TargetScan, DIANA, PITA, and mirSVR prediction tools. Separately, we obtained a miRNA expression array of 800 miRNAs in mature human peripheral blood NK cell populations defined as $CD56^{bright}CD94^{high}$ and $CD56^{dim}CD94^{low}$, which overlap significantly with $CD56^{bright}/CD16a^{-}$ and $CD56^{dim}/CD16a^{+}$ (Supplemental Fig. 1) (37). We screened for miRNAs that were highly expressed in $CD16a^{-}$ NK cells and poorly expressed in $CD16a^{+}$ NK cells. We next cross-referenced this list with the list of miRNAs compiled from the prediction tools and identified three miRNAs: miR-92a, miR-133a, and miR-218 (Fig. 4A). Each of these miRNAs has putative recognition sites in the 3′UTR of *FCGR3A*: miR-92a at UTR positions 255–262, miR-133a at UTR positions 458–471, and miR-218 at UTR positions 843–850 (Fig. 4B). We found that this pattern could be validated by real-time PCR in freshly sorted $CD16a^{-}$ and $CD16a^{+}$ primary NK cells for miR-133a and miR-218, but not for miR-92a (Fig. 4C).

To determine whether these putative miRNA regulators could interact with the 3′UTR of *FCGR3A* mRNA, we performed luciferase assays. We cloned the entire 3′UTR of *FCGR3A* into the luciferase vector pmirGLO downstream of the firefly *luc* gene, which is driven by a constitutively active promoter. Following cotransfection with an expression vector for one of each of the candidate miRNAs, we found that miR-218 showed a trend toward negative regulation of luciferase activity (Fig. 4D).

miR-218 is a negative regulator of CD16a in human NK cells

To validate the activity of miR-218 against *FCGR3A*, we overexpressed miR-218 in primary human NK cells by lentiviral infection. Transduced cells were sorted based on GFP expression and analyzed by flow cytometry for CD16 expression (Supplemental Fig. 2A). The average transduction efficiency (percentage of GFP^{+}) was 58.0 ± 23.9% for empty vector and 13.8 ± 9.2% for miR-218 (Supplemental Fig. 2B). We found that miR-218 overexpression resulted in decreased CD16a surface expression in NK cells infected with miR-218 virus compared with control virus (Fig. 5A, 5B). We confirmed that miR-218 virus-infected cells did overexpress miR-218 (Fig. 5C) and also found that this overexpression inversely correlated with *FCGR3A* mRNA expression (Fig. 5D).

Discussion

In this article, we describe two important modes of epigenetic control of CD16a expression in primary NK cells that involve regulation at the transcriptional and posttranscriptional levels. Previous articles have described that Pmed1-A promotes specific expression of *FCGR3A* in NK cells (23, 24, 35); however, sequence features alone cannot fully account for the lineage- and

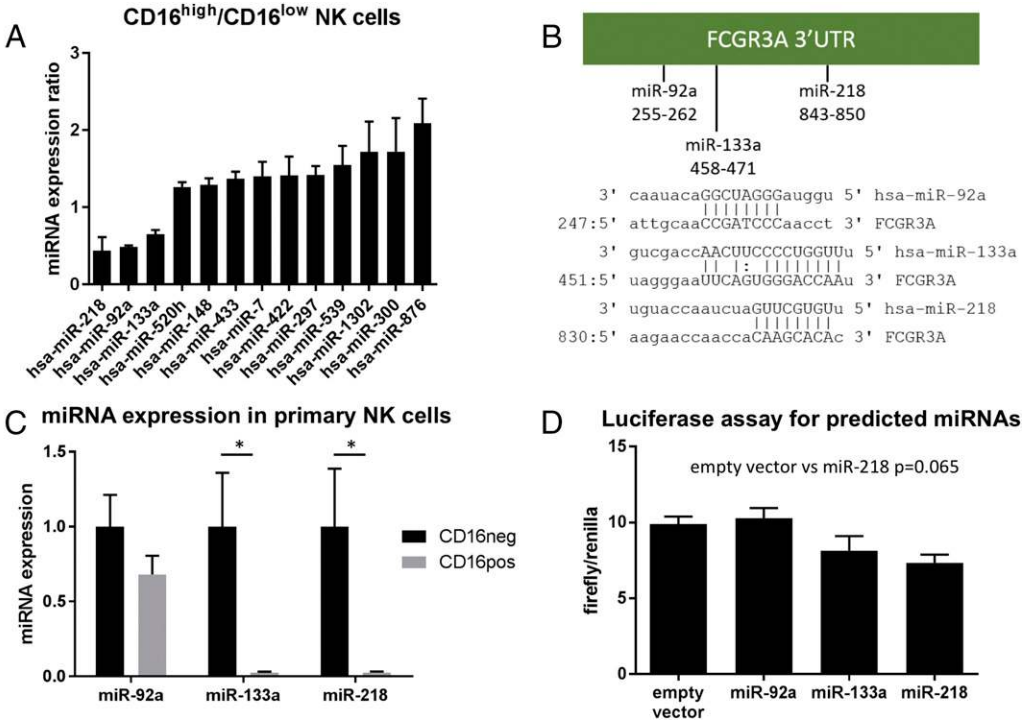

FIGURE 4. Identification of miR-218 as a potential regulator of *FCGR3A*. (**A**) Expression ratio of predicted miRNAs that were present in the miRNA expression array comparing CD16a$^+$ and CD16a$^-$ NK cells freshly isolated from adult peripheral blood. A ratio < 1 indicates low expression in CD16a$^+$ NK cells, whereas a ratio > 1 indicates high expression in CD16a$^+$ NK cells. (**B**) Predicted miRNA regulators of *FCGR3A* have putative binding sites in the *FCGR3A* 3′UTR. (**C**) Validation of expression of predicted miRNA regulators of *FCGR3A* by quantitative PCR ($n = 3$). (**D**) Luciferase expression as a ratio of firefly/*Renilla* for each expression vector ($n = 2$). Data are presented as mean ± SD. $*p < 0.05$.

stage-specific expression in primary cells. In our study, Pmed1-A and the immediate surrounding sequences were found to be the focal point of reduced methylation in CD16a$^+$ versus CD16a$^-$ NK cells, as well as in the CD16a$^+$ NK cell line NKL. Reduced Pmed1-A methylation was associated with expression of the *FCGR3A* variant 3 transcript, which initiates from Pmed1-A. Interestingly, Pprox-A displayed low methylation, regardless of CD16a expression, indicating that the initiation of *FCGR3A* variant 1 requires additional factor(s) that are not active in CD16a$^-$ NK cells. Indeed, previous work has shown that Pprox-A requires an enhancer element for activity (23, 24, 35). Based on the coordinated expression of *FCGR3A* variants 1 and 3, we propose that the unmethylated Pmed1-A may provide this function and enhance the expression of variant 1. In further support of the role of DNA methylation in the repression of FCGR3 genes, we made the novel observation that focally reduced methylation of Pprox-B was specifically associated with *FCGR3B* variant 1 expression in neutrophils. The lack of activity of Pprox-B in K562 luciferase experiments suggests that Pmed1-B may operate as an enhancer for Pprox-B; however, one cannot exclude that K562 cells are lacking the necessary transcriptional machinery to activate this promoter. Together, these findings indicate that a lineage-specific reduction in DNA methylation of key regulatory elements within the *FCGR3A* and *FCGR3B* promoter regions permits cell type–specific CD16a versus CD16b expression.

The activity state of a particular promoter or genomic element is dependent upon two primary factors: the epigenetic structure, which controls accessibility, and the presence of specific interacting *trans*-activating factors. We observed that the activity of Pmed1-A and Pmed1-B was restricted to YT and K562 cells, respectively, supporting the specific recognition of these sequences in NK and myeloid lineages, as found previously (23, 24, 35). These experiments reveal that YT cells, being of the NK lineage, possess the transcriptional machinery to selectively activate exogenous Pmed1-A; however, YT cells do not express endogenous *FCGR3A*, in concordance with the observation of high endogenous Pmed1-A methylation. Indeed, in vitro methylation of Pmed1-A silenced its activity. Because YT cells represent an earlier stage of NK development (38), our findings suggest that the transcriptional machinery required may already be active in earlier stages of NK cell development. We propose that Pmed1-A methylation prevents interaction with the transcriptional machinery and that Pmed1-A demethylation may function as the switch for CD16a expression during the transition from stage 4 to stage 5 NK development.

All sequence variations between Pmed1-A and Pmed1-B involve CpG dinucleotides. Interestingly, a greater number of CpGs are retained in the Pmed1-A region compared with Pmed1-B, concomitant with the greater importance of Pmed1-A for *FCGR3A* than for *FCGR3B* in NK cells. Conversely, the Pprox-B promoter that is primarily used by neutrophils retains two CpGs not present in Pprox-A. Remarkably, mutation of one or two variant CpGs in Pmed1 was sufficient to disrupt the lineage specificity of wild-type Pmed1-A and Pmed1-B sequences. These findings highlight the dual importance of CpGs in the Pmed1 region, functioning as an off switch when methylated and concurrently endowing selective activity when unmethylated.

In our survey of miRNA expression in peripheral blood–derived NK cells, we found that the majority of differentially expressed miRNAs were more highly expressed in the mature CD16a$^+$ NK cell population than in the less mature CD16a$^-$ population. This greatly narrowed our search for putative direct negative regulators of *FCGR3A* mRNA. For three miRNAs, we observed consistent, but modest, differences in miRNA expression between CD16a$^-$ and CD16a$^+$ NK cells. Direct validation of miR-218 expression in CD16a$^+$ and CD16a$^-$ primary NK cells demonstrated significant differences in relative expression levels. This difference in scale may be due, in part, to differences in experimental technique, as well as to

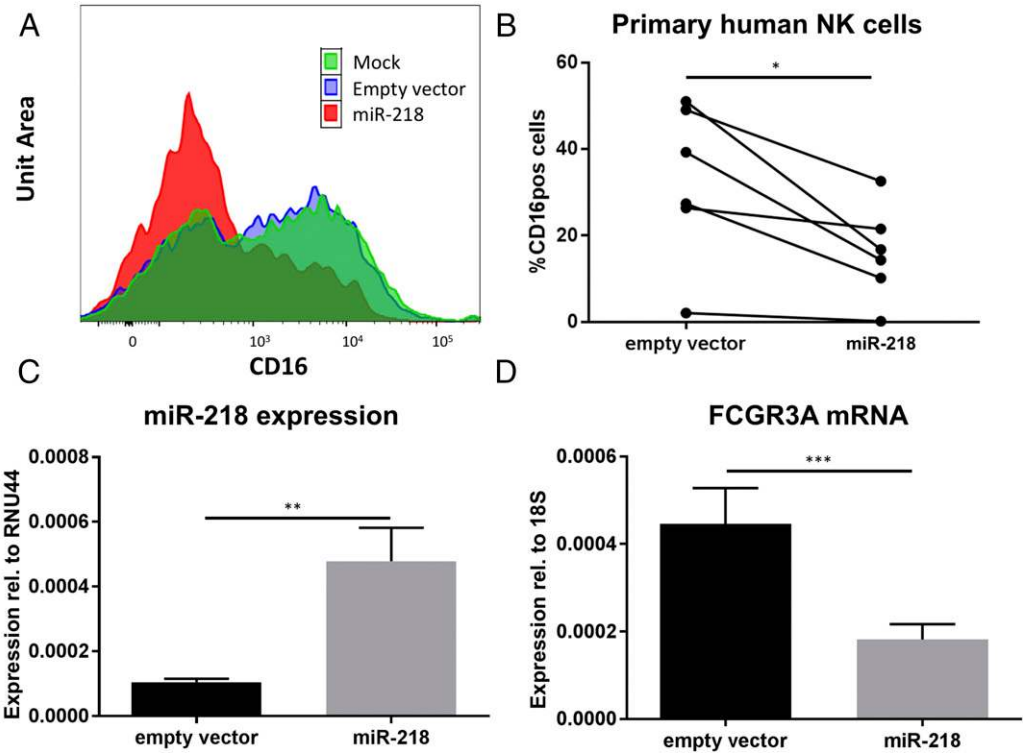

FIGURE 5. miR-218 negatively regulates CD16a in primary human NK cells. Primary human NK cells were enriched by magnetic selection to >70% purity and infected with lentivirus containing miR-218 or empty vector. Forty-eight hours postinfection, NK cells were sorted as live/CD3$^-$/CD56$^+$/GFP$^+$ lymphocytes. (**A**) Representative line graph (of one of six donors) of CD16a expression in live/CD3$^-$/CD56$^+$/GFP$^+$ primary human NK cells infected with miR-218 or empty vector virus. (**B**) CD16a expression in primary human NK cells infected with miR-218 or empty vector virus. (**C**) Validation of miR-218 overexpression by real-time PCR. (**D**) *FCGR3A* mRNA expression assessed by real-time RT-PCR in sorted NK cells infected with miR-218 or empty vector. (B–D) Data are mean ± SD, $n = 6$. *$p = 0.05$, **$p < 0.01$, ***$p < 0.005$.

partly overlapping populations. CD56^{bright}/CD94^{hi} NK cells correspond in many ways to CD16a$^-$ stage 4 NK cells, but they have some level of CD16a (9, 37). This would explain the modest differences in miRNA expression between NK populations in the expression array and the stark differences in the direct validation by quantitative PCR using CD16a$^-$ and CD16a$^+$ NK cells. In addition to the difference in miR-218 expression between CD16a$^+$ and CD16a$^-$ NK cells, we further observed direct antagonism of miR-218 against CD16a with overexpression studies in primary NK cells. These results suggest that a layer of miRNA regulation functions in conjunction with *FCGR3A* methylation–based silencing, potentially for the purpose of controlling spurious transcription that may occur despite promoter repression.

In summary, we propose a system of regulation of FCGR3 homologs that confers profound cell-type specificity, despite minimal differences in regulatory sequences, and facilitates strong and fine regulation of *FCGR3A* expression in NK cells. We have found that well-defined genetic elements with distinct regulatory functions cooperate with epigenetic modifications to ultimately control the cell type–specific expression. This knowledge may provide avenues for improving NK-dependent antitumor strategies, such as ADCC-based therapeutics and the use of engineered NK cells.

Disclosures

The authors have no financial conflicts of interest.

References

1. Clynes, R. A., T. L. Towers, L. G. Presta, and J. V. Ravetch. 2000. Inhibitory Fc receptors modulate in vivo cytotoxicity against tumor targets. *Nat. Med.* 6: 443–446.
2. Weng, W. K., and R. Levy. 2003. Two immunoglobulin G fragment C receptor polymorphisms independently predict response to rituximab in patients with follicular lymphoma. *J. Clin. Oncol.* 21: 3940–3947.
3. Anegón, I., M. C. Cuturi, G. Trinchieri, and B. Perussia. 1988. Interaction of Fc receptor (CD16) ligands induces transcription of interleukin 2 receptor (CD25) and lymphokine genes and expression of their products in human natural killer cells. *J. Exp. Med.* 167: 452–472.
4. Carter, P., L. Presta, C. M. Gorman, J. B. Ridgway, D. Henner, W. L. Wong, A. M. Rowland, C. Kotts, M. E. Carver, and H. M. Shepard. 1992. Humanization of an anti-p185HER2 antibody for human cancer therapy. *Proc. Natl. Acad. Sci. USA* 89: 4285–4289.
5. Lewis, G. D., I. Figari, B. Fendly, W. L. Wong, P. Carter, C. Gorman, and H. M. Shepard. 1993. Differential responses of human tumor cell lines to anti-p185HER2 monoclonal antibodies. *Cancer Immunol. Immunother.* 37: 255–263.
6. Freud, A. G., J. Yu, and M. A. Caligiuri. 2014. Human natural killer cell development in secondary lymphoid tissues. *Semin. Immunol.* 26: 132–137.
7. Freud, A. G., and M. A. Caligiuri. 2006. Human natural killer cell development. *Immunol. Rev.* 214: 56–72.
8. Chan, A., D. L. Hong, A. Atzberger, S. Kollnberger, A. D. Filer, C. D. Buckley, A. McMichael, T. Enver, and P. Bowness. 2007. CD56bright human NK cells differentiate into CD56dim cells: role of contact with peripheral fibroblasts. *J. Immunol.* 179: 89–94.
9. Freud, A. G., A. Yokohama, B. Becknell, M. T. Lee, H. C. Mao, A. K. Ferketich, and M. A. Caligiuri. 2006. Evidence for discrete stages of human natural killer cell differentiation in vivo. *J. Exp. Med.* 203: 1033–1043.
10. Cassatella, M. A., I. Anegón, M. C. Cuturi, P. Griskey, G. Trinchieri, and B. Perussia. 1989. Fc gamma R(CD16) interaction with ligand induces Ca2+ mobilization and phosphoinositide turnover in human natural killer cells. Role of Ca2+ in Fc gamma R(CD16)-induced transcription and expression of lymphokine genes. *J. Exp. Med.* 169: 549–567.
11. Harris, D. T., W. W. Travis, and H. S. Koren. 1989. Induction of activation antigens on human natural killer cells mediated through the Fc-gamma receptor. *J. Immunol.* 143: 2401–2406.
12. Ortaldo, J. R., A. T. Mason, and J. J. O'Shea. 1995. Receptor-induced death in human natural killer cells: involvement of CD16. *J. Exp. Med.* 181: 339–344.
13. Ravetch, J. V., and S. Bolland. 2001. IgG Fc receptors. *Annu. Rev. Immunol.* 19: 275–290.
14. Smyth, M. J., E. Cretney, J. M. Kelly, J. A. Westwood, S. E. Street, H. Yagita, K. Takeda, S. L. van Dommelen, M. A. Degli-Esposti, and Y. Hayakawa. 2005. Activation of NK cell cytotoxicity. *Mol. Immunol.* 42: 501–510.
15. Sondel, P. M., and J. A. Hank. 2001. Antibody-directed, effector cell-mediated tumor destruction. *Hematol. Oncol. Clin. North Am.* 15: 703–721.
16. Alderson, K. L., and P. M. Sondel. 2011. Clinical cancer therapy by NK cells via antibody-dependent cell-mediated cytotoxicity. *J. Biomed. Biotechnol.* 2011: 379123.

17. Trotta, R., K. A. Puorro, M. Paroli, L. Azzoni, B. Abebe, L. C. Eisenlohr, and B. Perussia. 1998. Dependence of both spontaneous and antibody-dependent, granule exocytosis-mediated NK cell cytotoxicity on extracellular signal-regulated kinases. *J. Immunol.* 161: 6648–6656.
18. Perussia, B. 1998. Fc receptors on natural killer cells. *Curr. Top. Microbiol. Immunol.* 230: 63–88.
19. Romee, R., B. Foley, T. Lenvik, Y. Wang, B. Zhang, D. Ankarlo, X. Luo, S. Cooley, M. Verneris, B. Walcheck, and J. Miller. 2013. NK cell CD16 surface expression and function is regulated by a disintegrin and metalloprotease-17 (ADAM17). *Blood* 121: 3599–3608.
20. Matsuo, Y., and H. G. Drexler. 2003. Immunoprofiling of cell lines derived from natural killer-cell and natural killer-like T-cell leukemia-lymphoma. *Leuk. Res.* 27: 935–945.
21. Li, M., U. Wirthmueller, and J. V. Ravetch. 1996. Reconstitution of human Fc gamma RIII cell type specificity in transgenic mice. *J. Exp. Med.* 183: 1259–1263.
22. Fossati, G., R. J. Moots, R. C. Bucknall, and S. W. Edwards. 2002. Differential role of neutrophil Fcgamma receptor IIIB (CD16) in phagocytosis, bacterial killing, and responses to immune complexes. *Arthritis Rheum.* 46: 1351–1361.
23. Gessner, J. E., T. Grussenmeyer, W. Kolanus, and R. E. Schmidt. 1995. The human low affinity immunoglobulin G Fc receptor III-A and III-B genes. Molecular characterization of the promoter regions. *J. Biol. Chem.* 270: 1350–1361.
24. Gessner, J. E., T. Grussenmeyer, M. Dumbsky, and R. E. Schmidt. 1996. Separate promoters from proximal and medial control regions contribute to the natural killer cell-specific transcription of the human FcgammaRIII-A (CD16-A) receptor gene. *J. Biol. Chem.* 271: 30755–30764.
25. Bröske, A. M., L. Vockentanz, S. Kharazi, M. R. Huska, E. Mancini, M. Scheller, C. Kuhl, A. Enns, M. Prinz, R. Jaenisch, et al. 2009. DNA methylation protects hematopoietic stem cell multipotency from myeloerythroid restriction. *Nat. Genet.* 41: 1207–1215.
26. Trowbridge, J. J., J. W. Snow, J. Kim, and S. H. Orkin. 2009. DNA methyltransferase 1 is essential for and uniquely regulates hematopoietic stem and progenitor cells. *Cell Stem Cell* 5: 442–449.
27. Ferlazzo, G., D. Thomas, S. L. Lin, K. Goodman, B. Morandi, W. A. Muller, A. Moretta, and C. Münz. 2004. The abundant NK cells in human secondary lymphoid tissues require activation to express killer cell Ig-like receptors and become cytolytic. *J. Immunol.* 172: 1455–1462.
28. Vitale, C., L. Chiossone, G. Morreale, E. Lanino, F. Cottalasso, S. Moretti, G. Dini, L. Moretta, and M. C. Mingari. 2004. Analysis of the activating receptors and cytolytic function of human natural killer cells undergoing in vivo differentiation after allogeneic bone marrow transplantation. *Eur. J. Immunol.* 34: 455–460.
29. Ehrich, M., M. R. Nelson, P. Stanssens, M. Zabeau, T. Liloglou, G. Xinarianos, C. R. Cantor, J. K. Field, and D. van den Boom. 2005. Quantitative high-throughput analysis of DNA methylation patterns by base-specific cleavage and mass spectrometry. *Proc. Natl. Acad. Sci. USA* 102: 15785–15790.
30. Kent, W. J., C. W. Sugnet, T. S. Furey, K. M. Roskin, T. H. Pringle, A. M. Zahler, and D. Haussler. 2002. The human genome browser at UCSC. *Genome Res.* 12: 996–1006.
31. Weigel, C., M. R. Veldwijk, C. C. Oakes, P. Seibold, A. Slynko, D. B. Liesenfeld, M. Rabionet, S. A. Hanke, F. Wenz, E. Sperk, et al. 2016. Epigenetic regulation of diacylglycerol kinase alpha promotes radiation-induced fibrosis. *Nat. Commun.* 7: 10893.
32. Wei, Q. X., R. Claus, T. Hielscher, D. Mertens, A. Raval, C. C. Oakes, S. M. Tanner, A. de la Chapelle, J. C. Byrd, S. Stilgenbauer, and C. Plass. 2013. Germline allele-specific expression of DAPK1 in chronic lymphocytic leukemia. *PLoS One* 8: e55261.
33. Briercheck, E. L., R. Trotta, L. Chen, A. S. Hartlage, J. P. Cole, T. D. Cole, C. Mao, P. P. Banerjee, H. T. Hsu, E. M. Mace, et al. 2015. PTEN is a negative regulator of NK cell cytolytic function. *J. Immunol.* 194: 1832–1840.
34. Gessner, J. E., T. Grussenmeyer, and R. E. Schmidt. 1995. Differentially regulated expression of human IgG Fc receptor class III genes. *Immunobiology* 193: 341–355.
35. Heusohn, F., G. Wirries, R. E. Schmidt, and J. E. Gessner. 2002. The Pmed1 gene promoter of human Fc gamma RIIIA can function as a NK/T cell-specific restriction element, which involves binding of Sp1 transcription factor. *J. Immunol.* 168: 2857–2864.
36. Witkos, T. M., E. Koscianska, and W. J. Krzyzosiak. 2011. Practical aspects of microRNA target prediction. *Curr. Mol. Med.* 11: 93–109.
37. Yu, J., H. C. Mao, M. Wei, T. Hughes, J. Zhang, I. K. Park, S. Liu, S. McClory, G. Marcucci, R. Trotta, and M. A. Caligiuri. 2010. CD94 surface density identifies a functional intermediary between the CD56bright and CD56dim human NK-cell subsets. *Blood* 115: 274–281.
38. Yodoi, J., K. Teshigawara, T. Nikaido, K. Fukui, T. Noma, T. Honjo, M. Takigawa, M. Sasaki, N. Minato, M. Tsudo, et al. 1985. TCGF (IL 2)-receptor inducing factor(s). I. Regulation of IL 2 receptor on a natural killer-like cell line (YT cells). *J. Immunol.* 134: 1623–1630.